Energy bands in ferromagnetic iron*

J. Callaway and C. S. Wang†
Department of Physics and Astronomy, Louisiana State University, Baton Rouge, Louisiana 70803
(Received 21 March 1977)

Energy bands in ferromagnetic iron have been calculated self-consistently using three different potentials. The first is the Kohn-Sham-Gaspar local-exchange approximation; second, a similar potential used in a previous calculation ($X\alpha$ with $\alpha = 0.64$); third, the spin-polarized exchange-correlation potential of von Barth and Hedin. The linear-combination-of-atomic-orbitals method was employed using a basis set of independent Gaussian orbitals. Spin-orbit coupling and other relativistic effects were ignored. Results are presented for the Fermi surface, charge and spin form factors, contact charge and spin densities, and the Compton profile. Use of the exchange-correlation potential leads to improvement of calculated results in comparison with experiment, but some discrepancies still remain.

I. INTRODUCTION

This paper presents the results of a self-consistent calculation of energy bands in ferromagnetic iron using the linear-combination-of-atomic-orbitals (LCAO) method with a basis consisting of independent Gaussian functions. This work parallels a previous report concerning nickel,[1] and contains several improvements in computational methods with respect to our previous calculations for iron.[2,3] These improvements are described in Ref. 1. A major emphasis here is the following question: How are the results of a spin-polarized band calculation using a local-exchange potential affected by the inclusion of some correlation effects by means of the more-sophisticated exchange-correlation potential of von Barth and Hedin[4]? This question is studied by the comparison of results of three self-consistent calculations using identical computational procedures. In addition, we present a detailed description of the iron Fermi surface calculated using the exchange-correlation potential. Electron charge and spin densities at a nuclear site are calculated. These results include the modification of core-electron wave functions in the crystal environment. The difference between the Compton profiles of majority- and minority-spin electrons has also been obtained: experimental results for this quantity have recently been reported.[5] Spin-orbit coupling and other relativistic correlations are neglected in the present work.

This paper is organized as follows: The remainder of this section contains a brief description of the potentials employed and the computational methods. The results for the band structures and density of states are presented in Sec. II. The charge and spin densities at a nuclear site are given in Sec. III; the corresponding form factors are in Sec. IV. The Fermi surface is described in Sec. V, and the Compton profile in Sec. VI. Some conclusions are offered in Sec. VII.

Two of the calculations we shall describe below include a local-exchange potential of the form

$$V_{x,\sigma} = -3e^2\alpha[(3/4\pi)\rho_\sigma]^{1/3}. \tag{1}$$

We have considered the cases following: (i) $\alpha = \frac{2}{3}$ [the Kohn-Sham-Gaspar[6,7] (KSG) value]; (ii) $\alpha = 0.64$, an empirically chosen value in previous calculations.[2,3] We repeated this work in order to see if the results would be significantly altered by the use of improved computational techniques. They were not. The third calculation employed the von Barth–Hedin exchange-correlation potential[4] (abbreviated vBH)

$$V_{xc,\sigma} = A(\rho)(\rho_\sigma/\rho)^{1/3} + B(\rho), \tag{2}$$

where A and B are functions of the charge density which are given in parametrized form in Ref. 4. Comparison of results obtained from calculations (1) and (3) give some information as to the effect of that portion of the electron interaction included in the one-particle potential (2), while our second case tests the extent to which our previous results are changed by improved computational procedures.

We shall indicate here only the most essential features of our computational methods. A detailed report describing the computer programs can be obtained from the authors and will be submitted for publication elsewhere.[8] The calculation employs a basis of localized functions which are independent Gaussian orbitals: 13 s-type orbitals, 10 p-type, 5 d, and 1 f. When the possible angular dependences are included, the Hamiltonian matrix has the dimension 75×75 at a general point in the Brillouin zone. The orbital exponents which define the Gaussians are the same as those used by Wachters in an atomic self-consistent calculation,[9] except that the s and p orbitals of longest range have been de-

leted. The exponent of the f orbital was chosen to be 0.9. The use of independent Gaussian orbitals permits the core wave functions to adjust to the crystal potential, and this makes possible accurate calculations of spin and charge densities. The charge and spin densities used to start the iterative cycle were those of a lattice of neutral iron atoms in the d^7s^1 configuration, with 4.6 majority-spin d electrons and 2.4 of minority spin. Wave functions from Wachters's calculation[9] were employed to construct those densities.

In the course of the self-consistent calculations, the charge density was sampled at 91 points in $\frac{1}{48}$th of the Brillouin zone. The iteration process was terminated when the change in the (110), (200), and (211) Fourier coefficients of both the Coulomb and exchange potentials was less than about 0.0004 Ry. The energy levels of interest appear to be stable at this point to about 0.001 Ry in most cases. For $\alpha = \frac{2}{3}$, convergence was slow due to the closeness of the Fermi energy to the majority-spin H_{25}' state, and the calculation was terminated when the change in the coefficients mentioned was 0.001 Ry. After the completion of self-consistency, energy levels and wave functions were calculated at 506 points in $\frac{1}{48}$ of the zone for the vBH and $\alpha = 0.64$ potentials.

II. BAND STRUCTURE AND DENSITY OF STATES

Reference 2 contains citations of previous band calculations for iron which we believe to be complete. Our present calculated energy values are listed in Table I for points of high symmetry. The band structure resulting from the vBH potential is shown in Fig. 1. All of our computations have been performed for a lattice constant $a = 5.4057$ (a.u.).

The most important of the calculations performed by other groups are those of Wakoh and Yamashita,[10] Duff and Das,[11] Yasui *et al.*,[12] and Janak and Williams.[13] These calculations involve both different calculational techniques and different exchange potentials (Wakoh and Yamashita use $\alpha = 0.5$; Yasui *et al.* use $\alpha = 0.656$; Janak and Williams use the von Barth–Hedin potential; while Duff and Das employ a different functional form of potential). We will not compare specific energy values, but would like rather to note good general agreement between the calculations reported here and those of Yasui *et al.* and Wakoh and Yamashita (except that as a consequence of their use of $\alpha = 0.5$, the latter authors obtain consistently smaller exchange splittings of d states than we do). On the other hand, our results differ quite substantially from those of Duff and Das. Their results for

TABLE I. Energies of the lowest six bands at symmetry points of the zone: ↑ indicates majority spin; ↓ minority spin. The number in parentheses following the energy designates the symmetry of the state.

Fe Potential	Band	Energies at symmetry points $\Gamma_\uparrow$	$\Gamma_\downarrow$	$H_\uparrow$	$H_\downarrow$	$P_\uparrow$	$P_\downarrow$	$N_\uparrow$	$N_\downarrow$
vBH	1	−1.1649(1)	−1.1526(1)	−0.8928(12)	−0.7818(12)	−0.7951(4)	−0.6964(4)	−0.9111(1)	−0.8266(1)
vBH	2	−0.7270(25′)	−0.5931(25′)	−0.8928(12)	−0.7818(12)	−0.7951(4)	−0.6969(4)	−0.8022(2)	−0.6807(2)
vBH	3	−0.7270(25′)	−0.5931(25′)	−0.5534(25′)	−0.3984(25′)	−0.7951(4)	−0.6969(4)	−0.6253(1)	−0.5206(1′)
vBH	4	−0.7270(25′)	−0.5931(25′)	−0.5534(25′)	−0.3984(25′)	−0.6010(3)	−0.4461(3)	−0.6123(4)	−0.4700(1)
vBH	5	−0.6251(12)	−0.4651(12)	−0.5534(25′)	−0.3984(25′)	−0.6010(3)	−0.4461(3)	−0.5341(3)	−0.4488(4)
vBH	6	−0.6251(12)	−0.4651(12)	+0.1411(15)	+0.1616(15)	+0.0527(4)	−0.1206(4)	−0.5324(1′)	−0.3765(3)
vBH					$E_F = -0.5618$				
KS	1	−1.0184(1)	−1.0095(1)	−0.7524(12)	−0.6156(12)	−0.6540(4)	−0.5338(4)	−0.7695(1)	−0.6666(1)
KS	2	−0.5872(25′)	−0.4182(25′)	−0.7524(12)	−0.6156(12)	−0.6540(4)	−0.5338(4)	−0.6621(2)	−0.5092(2)
KS	3	−0.5872(25′)	−0.4182(25′)	−0.4136(25′)	−0.2179(25′)	−0.6540(4)	−0.5338(4)	−0.4857(1)	−0.3802(1′)
KS	4	−0.5872(25′)	−0.4182(25′)	−0.4136(25′)	−0.2179(25′)	−0.4706(3)	−0.2652(3)	−0.4729(4)	−0.2907(1)
KS	5	−0.4856(12)	−0.2853(12)	−0.4136(25′)	−0.2179(25′)	−0.4706(3)	−0.2652(3)	−0.3943(3)	−0.2680(4)
KS	6	−0.4856(12)	−0.2853(12)	+0.2844(15)	+0.3052(15)	+0.1965(4)	+0.2781(4)	−0.3874(1′)	−0.1954(3)
KS					$E_F = -0.4166$				
$\alpha = 0.64$	1	−0.9909(1)	−0.9866(1)	−0.7180(12)	−0.5898(12)	−0.6190(4)	−0.5076(4)	−0.7363(1)	−0.6415(1)
$\alpha = 0.64$	2	−0.5496(25′)	−0.3899(25′)	−0.7180(12)	−0.5898(12)	−0.6190(4)	−0.5076(4)	−0.6257(2)	−0.4818(2)
$\alpha = 0.64$	3	−0.5496(25′)	−0.3899(25′)	−0.3738(25′)	−0.5898(25′)	−0.6190(4)	−0.5076(4)	−0.4470(1)	−0.3566(1′)
$\alpha = 0.64$	4	−0.5496(25′)	−0.3899(25′)	−0.3738(25′)	−0.1879(25′)	−0.4315(3)	−0.2359(3)	−0.4338(4)	−0.2617(1)
$\alpha = 0.64$	5	−0.4469(12)	−0.2564(12)	−0.3738(25′)	−0.1879(25′)	−0.4315(3)	−0.2359(3)	−0.3592(1′)	−0.2338(4)
$\alpha = 0.64$	6	−0.4469(12)	−0.2564(12)	+0.3132(15)	+0.3291(15)	+0.2292(4)	+0.3051(4)	−0.3542(3)	−0.1651(3)
$\alpha = 0.64$					$E_F = -0.3791$				

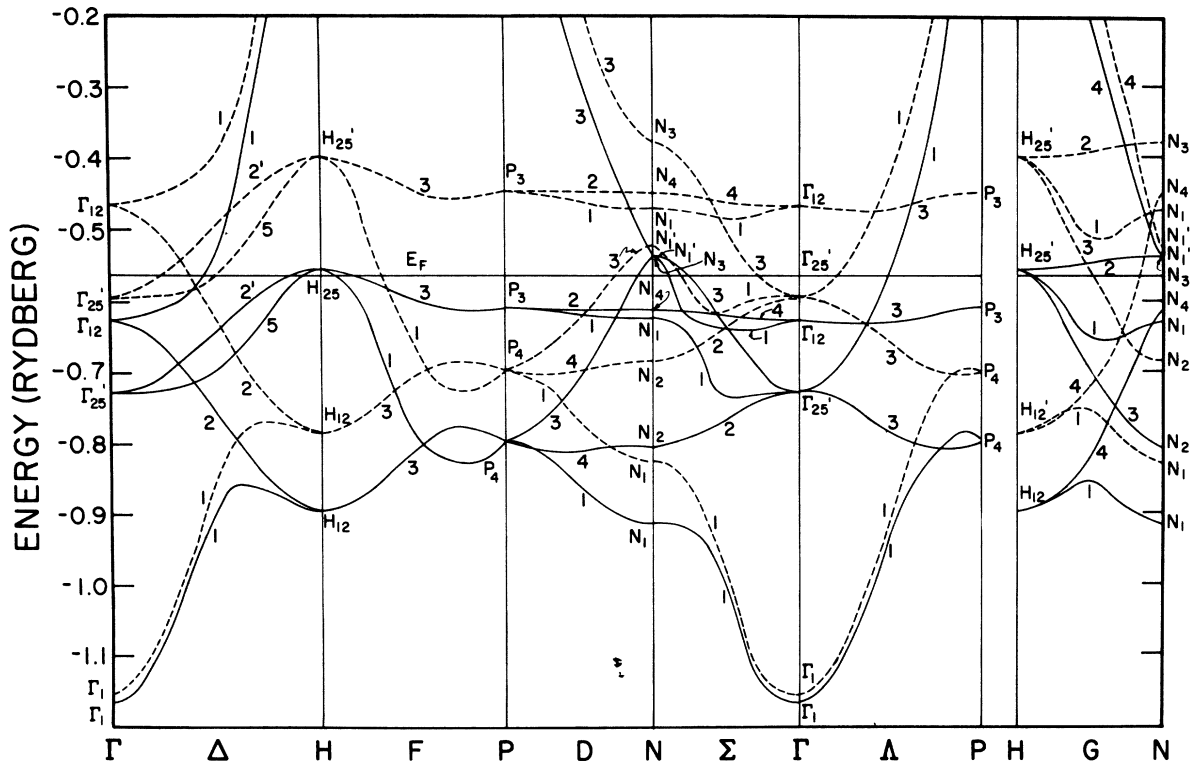

FIG. 1. Energy bands in ferromagnetic iron along some lines of high symmetry according to the vBH potential. Solid lines are majority-spin states, dashed are minority-spin states.

both the overall band width (about 8 eV for a single-spin subband) and the exchange splitting (about 3.5 eV) are significantly larger than those reported here. Janak and Williams do not present details of their band structure. Comparisons of other results of different calculations will be presented in other sections.

The following discussion emphasizes the comparison of results from the vBH potential with those based on the KSG ($\alpha = \frac{2}{3}$) potential. The $\alpha = 0.64$ bands are only slightly changed with respect to those from the KSG potential. The width of the occupied portion of the d bands is roughly characterized by the quantity $E_F - E(N_{1\uparrow})$. This does not vary much between the calculations [about 4.7 eV for the vBH potential, 4.8 eV for Kohn-Sham (KS)]. The width of the d bands including unoccupied portions is estimated by the difference $E(N_3) - E(N_1)$, the lowest N_1 level being used. We find, for the majority spins, a width of 5.1 eV for both the vBH and KS potentials. The minority spin bands are significantly wider (6.1 eV for the vBH potential, 6.4 for KS). The exchange splitting varies substantially over the d band, ranging from 1.3 eV (near the bottom of the band) to 2.2 eV near the top in the case of the vBH potential; the corresponding numbers for the KS potential are 1.6 and 2.7 eV. The common approximation of a constant d-band splitting, while reasonably appropriate for nickel,[8] is evidently rather poorly obeyed in iron. The exchange splitting of predominately s (and p) like states is much smaller than for d states, and larger for the vBH potential (0.2 eV for Γ and N_1') than for the KS potential (about 0.1 eV for the same states).

It should also be noted that portions of the d bands in the zone face (notably $P_3 - N_4$) are rather flat. A similar feature is present in nickel. This gives rise to a sharp peak in the density of states, as will be seen below.

The density of states was constructed (and the Fermi energy was determined) using the linear analytic tetrahedron method.[14-16] Our results based on the von Barth–Hedin potential are shown in Fig. 2. The other potentials lead to quite similar curves. Results for the density of states at the Fermi surface and magneton number are presented in Table II (experimental values[17,18] are also given). The characteristic spin splitting Δ, also presented there, is the separation of the majority- and minority-spin peaks in the density of states. The vBH potential leads to a slightly higher value

of $N(E_F)$; however, the discrepancy in comparison with the experimental value, which is larger by a factor of about 1.87 is quite substantial. Some of this may be attributed to phonon enhancement; however an 87% phonon enhancement would be unusually large. Edwards has suggested that a many-body effect resulting from the energy dependence of the self-energy may be responsible.[19]

The calculated magneton numbers are slightly larger than the experimental result. The saturation magnetization is given in Ref. 17 as 2.216, but this should be multiplied by $2/g$ ($g=2.09$) to eliminate the orbital magnetization. However, it should be noted that the departure of g from 2 is due to spin-orbit coupling; an effect not included in the present calculations. Our value for μ_B^* is in good agreement with that (2.17) obtained by Janak and Williams[13] who used the same form of potential; however, their result pertains to their calculated equilibrium lattice constant.

There are no experiments which measure directly the density of states away from the Fermi energy. However, measurements of the energy distribution of photoemitted electrons are frequently interpreted in terms of the density of states. This is reasonable for large scale structural which cannot be masked by matrix elements or escape effects. Pessa, Heimann, and Neddermeyer, have interpreted their observations of photoemission in terms of a sharp rise in the density of states 0.58 eV below the Fermi energy.[20] Our calculations yield a sharp peak about 0.6 eV below the Fermi level (vBH potential). The other calculations place the rise further below E_F. The position of a second maximum in the photoemission intensity 2.4 eV below E_F correlates rather well with our density of states.

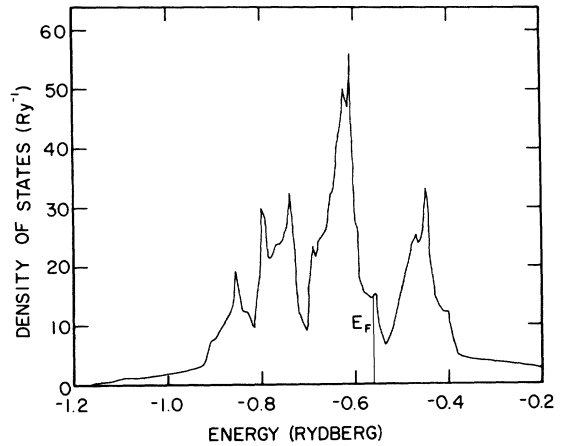

FIG. 2. Density of states including both majority and minority spins.

TABLE II. Magneton number μ_B^* density of states at the Fermi energy (E_F) in units of electrons/atom Ry for majority (↑) and minority (↓) spins, their total, and the characteristic exchange splitting Δ. The experimental references are (a) Ref. 17 including a g factor of 2.09, (b) Ref. 18.

	μ_B^*	$N_\uparrow(E_F)$	$N_\downarrow(E_F)$	$N_{\text{total}}(E_F)$	Δ(eV)
vBH	2.16	11.29	3.35	14.64	2.18
KS	2.30	11.69	3.68	15.37	2.68
$\alpha=0.64$	2.25	11.31	3.10	14.40	2.56
Expt	2.12(a)			27.37(b)	

III. CONTACT CHARGE AND SPIN DENSITIES

This section reports the results of our calculation of charge and spin densities at a nuclear site. Our values will be compared with experimental findings. The problem of the spin density has been of major interest since it was determined that the effective hyperfine field at an iron nucleus was negative, or equivalently, that minority-spin electrons predominate.[21] There have been several calculations of the effective hyperfine field, some of which have considered isolated atoms or ions,[22-25] while others have studied wave functions in metallic iron.[26-28] In the present calculation the charge and spin densities are determined at 91 points in the Brillouin zone. The contribution of the core electrons is determined in parallel with that of the band electrons. The diagonalization of the Hamiltonian matrix on the basis of independent Gaussian orbitals yields core energies and wave functions as well as those for band states, and in this way the self-consistent calculation allows naturally for possible modification of the core wave functions in the crystal environment.

The use of Gaussian orbitals as the basis set for the expansion of the wave functions may cause some concern for the quality of the computed functions.

The unphysical behavior of Gaussian functions near a nuclear site leads to inaccuracies in wave functions which are only partially compensated by the use of a large basis set. In order to estimate the error involved we have compared $|\psi(0)|^2$ for the s states of the isolated atom from self-consistent Hartree-Fock calculations using a Gaussian basis[9] and a Slater orbital basis.[29] The difference between the results for $|\psi(0)|^2$ is in no case larger than 4%. We expect that the difference between Gaussian and Slater values of $|\psi(0)|^2$ should be nearly independent of spin direction so that the values of the net spin density or effective hyperfine field are not uncertain by more than the overall 4%.

TABLE III. Contact charge and spin densities (atomic units). The experimental references are (a) Ref. 31; (b) results of Ref. 3 reevaluated with $\delta_{4s} = -0.047$ (see text); (c) Ref. 32; (d) Ref. 30.

	State	$\lvert\psi_\uparrow(0)\rvert^2$	$\lvert\psi_\downarrow(0)\rvert^2$	$\lvert\psi_\uparrow(0)\rvert^2+\lvert\psi_\downarrow(0)\rvert^2$	$\lvert\psi_\uparrow(0)\rvert^2-\lvert\psi_\downarrow(0)\rvert^2$	$\lvert\psi_\uparrow(0)\rvert^2/\lvert\psi_\downarrow(0)\rvert^2-1$
vBH	1*s*	5195.787	5195.828	10391.615	−0.041	−0.000 008
vBH	2*s*	472.074	472.815	944.889	−0.741	−0.001 57
vBH	3*s*	68.661	68.152	136.813	+0.509	+0.007 46
vBH	3*p*-hyb	0.003	0.003	0.006	0.000	
vBH	Band	2.673	2.805	5.478	−0.133	−0.0471
vBH	Total	5739.198	5739.604	11478.802	−0.406 (−213)	
KS	1*s*	5166.281	5166.409	10332.690	−0.128	−0.000 025
KS	2*s*	469.861	470.722	940.583	−0.861	−0.001 83
KS	3*s*	68.367	67.834	136.202	+0.533	+0.007 86
KS	3*p*-hyb	0.002	0.003	0.006	−0.001	
KS	Band	2.324	2.522	4.846	−0.197	−0.0785
KS	Total	5706.836	5707.491	11414.326	−0.655 (−343)	
$\alpha=0.64$	1*s*	5163.453	5163.576	10327.029	−0.123	−0.000 024
$\alpha=0.64$	2*s*	468.964	469.792	938.756	−0.828	−0.001 76
$\alpha=0.64$	3*s*	68.261	67.749	136.010	+0.512	+0.007 55
$\alpha=0.64$	3*p*-hyb	0.002	0.003	0.006	−0.001	
$\alpha=0.64$	Band	2.355	2.541	4.896	−0.187	−0.0732
$\alpha=0.64$	Total	5703.035	5703.661	11406.697	−0.626 (−328)	
Expt.	1*s*					
	2*s*					−0.0063 ± 0.0015(a)
	3*s*					+0.0145 ± 0.0068(a)
	3*s*					+0.0163 ± 0.0068(b)
	3*p*-hyb					
	Band			5.53 ± 0.46(c)		
	Total				−0.6466 ± 0.0006(339.0 ± 0.3)(d)	

Our values for $\lvert\psi(0)\rvert^2$ according to different potentials are listed in Table III, in atomic units. In parentheses we give the corresponding hyperfine field in kilogauss. Experimental results[30-32] are indicated where they are available.

We will first discuss the hyperfine field. The overall agreements with experiment[25] is quite good for both the KS and $\alpha = 0.64$ potentials. It should be noted that the band contribution to the hyperfine field is found to be negative, in contradiction to the work of Duff and Das,[27,28] but in agreement with the calculation of Wakoh and Yamashita.[26] The effects of correlations, insofar as these are included in the von Barth–Hedin potential are to reduce the magnitude of the spin polarization of all the shells; however, the negative "band" plus 2*s* polarizations are reduced more than the positive 3*s* polarization. As a result, the vBH potential yields an effective hyperfine field which is substantially smaller in magnitude than is obtained from the KS potential.

It must be recalled that the present results do not include relativistic effects. Recent calculations[33] show that, even for iron, solutions of the Dirac equation lead to a much larger value of the effective $\lvert\psi(0)\rvert^2$ for *s* states (about a 30% increase) than is obtained in a nonrelativistic theory. A nonnegligible contribution from *p* states is also found. Hence one must be cautious in drawing any conclusions concerning the superiority of one or another potential from the comparison of the hyperfine field with experiment.

The other experimental results quoted come from Shinshara and Fujioka[32] who obtained the contact charge density of band electrons from a study of the internal conversion of γ rays, and from Song, Trooster, and Benczer-Koller[31] who studied the spin polarization of core electrons with a technique combining the Mössbauer effect with internal conversion electron spectroscopy. The agreement between our calculations and these experiments is rather spotty. The contact charge density of band electrons is in reasonable agreement with experiment, while our results for the contact spin density of 2*s* electrons is much smaller in magnitude (independent of the potential used in the calculation) than the reported experimental result. We understand that an improved experiment is in progress.

Some additional comments are useful in regard to the work of Song *et al.*[31] These authors determine a value for the quantity

$$\delta_{ns} = \lvert\psi_{ns\uparrow}(0)\rvert^2/\lvert\psi_{ns\downarrow}(0)\rvert^2 - 1$$

for the $2s$ and $3s$ states. An estimate of δ_{4s}, the corresponding quantity for the band states is required in order to extract δ_{3s} from their data. Song *et al.* considered two values for δ_{4s}: (i) $\delta_{4s}=0$, which leads to the result $\delta_{3s}=0.0145\pm0.068$ quoted in Table III, and (ii) $\delta=0.86$, a value attributed to Stearns,[34] which gives $\delta_{3s}=-0.0100\pm0.068$. We have reevaluated δ_{3s} using the data of Song *et al.* and our value from the vBH potential for δ_{4s}. We find $\delta_{3s}=0.0163\pm0.068$ (this value is also given in Table III). If we use δ_{4s} from the KS potential, then $\delta_{3s}=0.0174$. It is, of course, possible that local density potentials do not describe the polarization of core levels accurately: however, the results for δ_{ns} ought to be consistent with the total hyperfine field.

IV. CHARGE AND SPIN FORM FACTORS

We have obtained the charge and spin form factors from our calculations. The results for the charge form factor are displayed in Table IV, where they are compared with other theoretical results,[27,35,36] and with experimental measurements of several different experimental groups.[37-43] It is to be noted that two[40,41] of the experimental groups have reported values of the form factor which are significantly smaller than the others. Five of the groups have used x-ray techniques involving powder and crystalline samples. A sixth has employed electron diffraction,[42] and the larger values of the form factor obtained in this way lends support to the results of Refs. 37–39.

If we accept the conclusion that the results of Refs. 40 and 41 should be disregarded, then the theoretical values are in substantial agreement with each other and with experiment, except for the calculation of Duff and Das.[27] The scatter in the experimental data is still too large to permit a meaningful discrimination between other calculations.

Our results for the normalized spin form factor are shown in Table V, where they are compared with experimental results.[44] No estimate of the probable experimental error is available to us. Our results have been computed with (a) $g=2$, and (b) no allowance for an orbital contribution. However, the contribution from the spin polarization of the core electrons has been included. Both the departure of g from 2 and the orbital moment are results of spin-orbit coupling and may be consistently neglected in a theory which ignores this effect. The results are in rather good overall agreement with experiment. In contrast to the situation in nickel the form factor from the vBH potential agrees better with the experimental values for most values of $\vec{K}$ than the other potentials.

V. FERMI SURFACE

We have obtained cross sections of the Fermi surface in the (100), (110), and (111) planes. These are shown in Figs. 3, 4, and 5, respectively, as obtained from the band calculation using the vBH potential. Since our calculations do not include spin-orbit coupling, we do not find the hybridization of majority and minority spin states and the consequent avoided crossings of Fermi-surface sheets.[3] Because spin-orbit coupling is a small effect in $3d$ transition metals except where degeneracies are removed, the Fermi surface predicted in a calculation in which spin-orbit coupling is neglected will be changed by such coupling only in the vicinity of an avoided crossing. However, it is evident from the diagrams that there are many crossings, and it seems that spin-orbit coupling has a more important effect on the iron Fermi than is true in nickel.

A brief description of the eight pieces of Fermi surface is given in Table VI. This table gives the cross sectional areas in the (100), (110), and (111) planes in magnetic field units (MG) appropriate for comparison with de Haas–van Alphen measurements. The table also presents experimental areas.[45,46]

The Fermi surface we have obtained in this is quite similar (apart from the effects of spin-orbit coupling) to that we described in a previous publication.[3] The effects of correlation, insofar as they are included in the von Barth–Hedin potential, do not change the Fermi surface qualitatively in comparison with that which is formed when either local exchange (only) potential (Kohn-Sham-Gaspar or $\alpha=0.64$) is employed. The same situation prevails in nickel.[8]

The use of an exchange-correlation potential reduces the splitting of the bands and the magneton number in comparison to the exchange only poten-

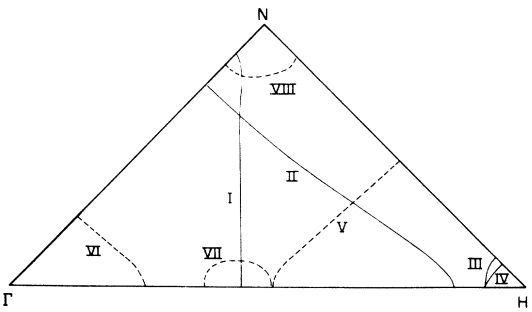

FIG. 3. Cross sections of the Fermi surface in a (100) plane according to the vBH potential. Majority-spin portions are represented by solid lines, minority by dashed lines. Refer to Table VI for a description of the surfaces.

TABLE IV. Charge-density form factor for iron according to the present calculations, other theoretical studies, and various experimental determinations.

Wave vector $a\vec{K}/2\pi$	Present calculations			Other theory						Experiment			
	vBH	KS	$\alpha=0.64$	Ref. 35	Ref. 27	Ref. 36	Ref. 37	Ref. 38	Ref. 39	Ref. 40	Ref. 41	Ref. 42	Ref. 43
(1,1,0)	18.295	18.267	18.225	18.34	17.59	18.371	18.19	18.39 ±0.44	18.38	17.63 ±0.20	17.54 ±0.25	18.34 ±0.07	
(2,0,0)	15.105	15.087	15.053	15.12	14.28	15.124	15.19 ±0.08	15.23 ±0.15	15.13	14.70 ±0.23	14.55 ±0.20	15.19 ±0.07	
(2,1,1)	13.074	13.061	13.035	12.99	12.55	13.033	13.01 ±0.08	13.09 ±0.17	13.18	12.62 ±0.21			
(2,2,0)	11.599	11.589	11.568	11.48	11.25	11.536	11.60 ±0.08	11.43 ±0.17	11.60	11.13 ±0.20			
(3,1,0)	10.474	10.466	10.449	10.36	10.35	10.409	10.47 ±0.05	10.45 ±0.13	10.39	10.10 ±0.19			
(2,2,2)	9.673	9.668	9.653	9.59	9.57	9.628		9.60 ±0.12		9.13 ±0.25			
(3,2,1)	9.023	9.019	9.007	8.96	8.84	8.977		9.00 ±0.14	8.97	8.75 ±0.10			
(4,0,0)	8.485	8.480	8.471	8.43	8.29	8.434							
(3,3,0)	8.111	8.108	8.099		8.00	8.078		8.00 ±0.10		7.68 ±0.21			
(4,1,1)	8.091	8.087	8.080		7.94	8.052		8.00 ±0.10		7.68 ±0.21			
Ratio (3,3,0) (4,1,1)	1.0025	1.0026	1.0024	1.0062	1.0076	1.0032					1.010		1.011 ±0.003
(4,2,0)	7.765	7.762	7.755			7.736		7.70 ±0.10					
(3,3,2)	7.503	7.502	7.495			7.487		7.32 ±0.10					
(4,2,2)	7.258	7.256	7.250			7.244		7.19 ±0.14					
(4,3,1)	7.052	7.051	7.045			7.045		6.99 ±0.12					
(5,1,0)	7.029	7.026	7.022			7.013		6.99 ±0.12					

TABLE V. Normalized-spin form factor for iron.

$\vec{K}$	Expt [a]	KS	$\alpha=0.64$	vBH
(0,0,0)	1.00	1.000	1.000	1.000
(1,1,0)	0.6347	0.6583	0.6573	0.6461
(2,0,0)	0.4077	0.4232	0.4230	0.4198
(2,1,1)	0.2520	0.2648	0.2629	0.2606
(2,2,0)	0.1751	0.1779	0.1762	0.1750
(3,1,0)	0.1383	0.1396	0.1400	0.1412
(2,2,2)	0.0620	0.0707	0.0682	0.0664
(3,2,1)	0.0461	0.0532	0.0520	0.0515
(4,0,0)	0.0711	0.0653	0.0674	0.0707
(3,3,0)	0.0132	0.0185	0.0175	0.0171
(4,1,1)	0.0376	0.0375	0.0384	0.0402
(4,2,0)	+0.0201	+0.0191	+0.0193	+0.0202
(3,3,2)	−0.0165	−0.0085	−0.0102	−0.0116
(4,2,2)	−0.0098	−0.0064	−0.0071	−0.0075
(4,3,1)	−0.0132	−0.0109	−0.0116	−0.0120
(5,1,0)	+0.0179	+0.0142	+0.0160	+0.0187
(5,2,1)	+0.0008	−0.0048	−0.0043	−0.0032
(4,4,0)	−0.0156	−0.0185	−0.0191	−0.0195
(4,3,3)	−0.0275	−0.0269	−0.0283	−0.0296
(5,3,0)	−0.0115	−0.0139	−0.0138	−0.0135
(4,4,2)	−0.0197	−0.0252	−0.0262	−0.0271
(6,0,0)	+0.0119	+0.0051	+0.0071	+0.0100
(5,3,2)	−0.0182	−0.0208	−0.0213	−0.0217
(6,1,1)	+0.0051	−0.0011	+0.0004	+0.0025
(6,2,0)	−0.0017	−0.0056	−0.0045	−0.0029
(5,4,1)	−0.0189	−0.0209	−0.0213	−0.0217
(6,2,2)	−0.0098	−0.0122	−0.0118	−0.0111

[a] Reference 42.

tials employed. This does lead to quantitative improvements in the agreement between theoretical and experimental Fermi surfaces, but some discrepancies remain. We comment below on the comparison between theory and experiment.

A. Large surfaces

Of the three predicted large surfaces (I, II, V; for notation see Table VI), two (I, V) have been observed. The agreement between theory and experiment is fairly good, but not excellent for these pieces. Surface II, the majority spin-hole arms requires further comment. We find that these arms extend across the Brillouin zone (in agreement with Ref. 10), but this contrasts with some other models.[46] Open orbits in [110] directions are observed in magnetoresistance experiments,[47,48] as is consistent with our results. However, in models where the arms are pinched off before reaching N, open orbits in the [110] direction can be obtained if magnetic breakdown is invoked. Open orbits are also observed in [100] directions.[47,48] These can be accommodated in our model only if extensive magnetic breakdown occurs. It should be observed that if the surface II arms are as found here there will be closed orbits around an arm in the vicinity of N in (110) and (111) planes. It is not clear to us whether any of the observed de Haas–van Alphen frequencies could be assigned to such orbits.

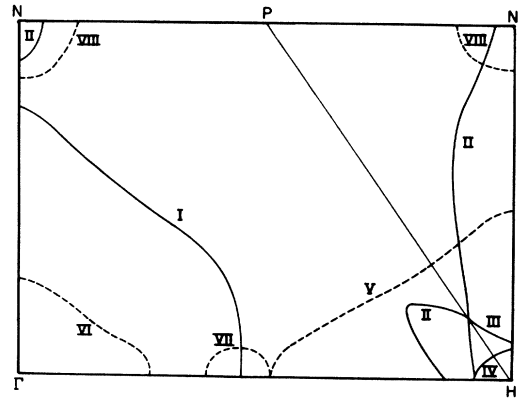

FIG. 4. Cross section of the Fermi surface in a (110) plane.

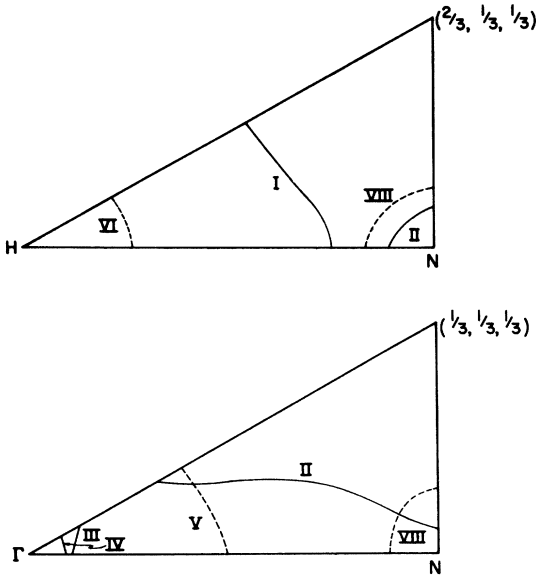

FIG. 5. Cross section of the Fermi surface in a (111) plane.

B. Medium-sized surfaces (VI, VII)

The area of the central minority spin-electron surface (VI) is in moderately good agreement with experiment. Surface VIII, the minority-spin hole pockets around N, has not been observed. Spin-orbit coupling can modify this surface substantially, however (see Ref. 3).

C. Small surfaces (III, IV, VII)

The present calculation apparently has great difficulty with the small surfaces. The majority-

TABLE VI. Fermi surface cross sectional areas expressed in frequency units (MG) appropriate to de Haas–van Alphen effect measurements. (a) Reference 45; (b) Ref. 46; (c) surface VII is described as a lens in Ref. 46; (d) in a Γ-centered plane; (e) in an *H*-centered plane.

Surface	Description	(100) plane Theor	(100) plane Expt	(110) plane Theor	(110) plane Expt	(111) plane Theor	(111) plane Expt
I	Large Γ-centered majority-spin electron surface	412	436 (a)	310	349 (a)	373	370 (a) 369 ± 4 (b)
II	Majority-spin hole surface (arms)			4.8		8.2	
III	Intermediate *H*-centered majority-spin hole pocket	9.4	20.6 (a) 23.8 (b)	15.5	33.4 (a)	12.2	27.0(a) 28.0± 0.2 (b)
IV	Small *H*-centered majority-spin hole pocket	7.0	15.0 (a) 21.0 (b)	6.9	12.3 (a) 12.0 ± 0.2 (b)	6.6	11.4 (a) 11.3 ± 0.2 (b)
V	*H*-centered large hole surface, minority	248	198 (a)	180	145 (a)	155	157 (a) 154 ± 1 (b)
VI	Central minority-spin electron surface	76	71 (a)	64	58 (a)	59	52.2 (a) 51.8 ± 0.6 (b)
VII	Minority-spin electron ball along Δ^c	5.4	3.85 (b, c) ±0.03	6.1	3.89 ± 0.03 (b, c)		4.11 ± 0.03(b, c)
VIII	Minority-spin hole pocket around *N*	16		19.6 (d) 15.8 (e)		19.2 (d) 15.4 (e)	

spin hole pockets at *H* (III, IV) are apparently much too small—this situation persists in all the calculations we have made. In addition, we obtain a small minority spin electron ball (VII) along the [100] axis. The area of this ball agrees moderately well with that assigned to a "lens" in Ref. 46; however, it should be emphasized that the model of Ref. 46 is quite different. In that work, the ball is much bigger, overlapping surface VI. Spin-orbit coupling then causes surfaces VI and VII to alter their connections, leaving a small lens and a protrusion on VI. This model has the added advantage of easily providing [100] open orbits. However, we have never been able to obtain such a model from our calculations.

In sum, the agreement between theory and experimental measurements of the Fermi surface is not as good as was found in nickel.[8] The iron Fermi surface is, however, much more complex than that of nickel. Perhaps alternative assignments of de Haas–van Alphen frequencies are possible.

VI. COMPTON PROFILE

In a previous calculation, we have obtained the Compton profile for ferromagnetic iron for directions of the momentum transfer $\vec{k}$ along the [100], [110], and [111] axis.[49] These calculations seem to be in reasonable agreement with the experiments.[50,51] A recent measurement has reported the difference between the Compton profiles of majority and minority spin electrons.[5] We have computed this quantity using our calculated wave functions based on the von Barth–Hedin potential. Additional corrections due to electron correlation may be present.[52] The general technique of the calculation are the same as in Ref. 49. Our results are shown in Fig. 6, where they are compared with the (normalized) experimental results.

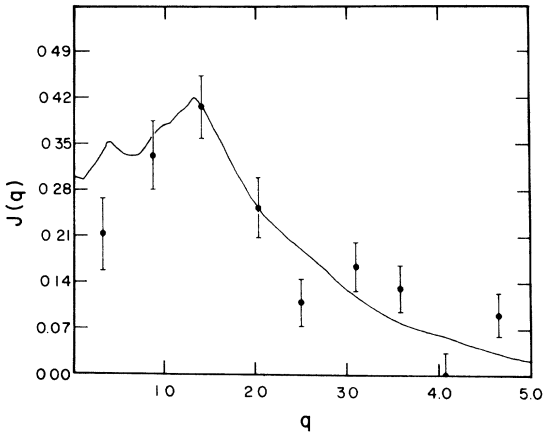

FIG. 6. Difference of the Compton profile for majority- and minority-spin electrons. The results are compared with the experimental values of Ref. 5. The experimental values have been normalized to the theoretical curve at $q = 1.4$.

The agreement is quite good except possibly for small values of the parameter q.

VII. CONCLUSIONS

We have presented results for energy bands, density of states, contact charge and spin densities, charge and spin form factors, the Fermi surface, and the difference between the Compton profile for majority and minority spin electrons in ferromagnetic iron. These properties have been studied on the basis of self-consistent calculations using local-exchange and exchange-correlation potentials.

The most important result is that there is substantial agreement between theory and experiment. There are certain nagging discrepancies whose precise significance is uncertain; notably the value of the density of states at the Fermi energy, and the areas of some small cross sections of the Fermi surface. However, band theory using local potentials is able to provide a reasonably quantitative account of most of the $T = 0$ °K electronic properties of iron; including not only the size but the spatial form of the magnetic moment. There is no evidence on the basis of the properties studied for exceptionally strong correlations which might require basic changes in the standard band picture.

Comparison of the results from the different calculations reported here, and including at least some of those reported by other authors indicates that the general agreement between theory and experiment is not particularly sensitive to the precise form of the exchange potential employed. Inclusion of some correlation effects in a local potential does not make major changes in the results, but does moderately improve the calculated Fermi surface.

As in the case of nickel, experimental investigation of the band structure has so far failed to provide us with one vital number which is required to determine the adequacy of these calculations: the average exchange splitting of the d bands. We have argued elsewhere that precise investigation of optical properties might furnish an answer to this question.

---

*Supported in part by the NSF.

†Present address: Dept. of Physics, Northwestern University, Evanston, Ill. 60201.

[1]C. S. Wang and J. Callaway, Phys. Rev. B 9, 4897 (1974).
[2]R. A. Tawil and J. Callaway, Phys. Rev. B 7, 4242 (1973).
[3]M. Singh, C. S. Wang, and J. Callaway, Phys. Rev. B 11, 287 (1975).
[4]U. von Barth and L. Hedin, J. Phys. C 5, 1629 (1972).
[5]N. Sakai and K. Ono, Phys. Rev. Lett. 37, 351 (1976).
[6]R. Gaspar, Acta Phys. Hung. 3, 263 (1964).
[7]W. Kohn and L. J. Sham, Phys. Rev. 140, A1133 (1965).
[8]C. S. Wang and J. Callaway, Phys. Rev. B 15, 298 (1977).
[9]A. J. H. Wachters, J. Chem. Phys. 52, 1033 (1970).
[10]S. Wakoh and J. Yamashita, J. Phys. Soc. Jpn. 21, 1712 (1966).
[11]K. J. Duff and T. P. Das, Phys. Rev. B 3, 192 (1971).
[12]M. Yasui, E. Hayashi, and M. Shimizu, J. Phys. Soc. Jpn. 34, 396 (1973).
[13]J. F. Janak and A. R. Williams, Phys. Rev. B 14, 4199 (1976).
[14]O. Jepsen and O. K. Andersen, Solid State Commun. 9, 1763 (1971); also, G. Lehman and M. Taut, Phys. Status Solidi B 54, 460 (1972).
[15]J. Rath and A. J. Freeman, Phys. Rev. B 11, 2109 (1975).
[16]S. P. Singhal, Phys. Rev. B 12, 564 (1975); 12, 6007 (1975).
[17]H. Danan, A. Herr, and A. J. P. Meyer, J. Appl. Phys. 39, 669 (1968).
[18]M. Dixon, F. E. Hoare, T. M. Holden, and D. E. Moody, Proc. R. Soc. Lond. A 285, 561 (1965).
[19]D. M. Edwards, Physica (Utr.) (to be published).
[20]M. Pessa, P. Heimann, and H. Neddermeyer, Phys. Rev. B 14, 3488 (1976).
[21]S. S. Hanna, J. Heberle, G. J. Perlow, R. S. Preston, and D. H. Vincent, Phys. Rev. Lett. 4, 513 (1960).
[22]J. H. Wood and G. W. Pratt, Phys. Rev. 107, 995 (1957).
[23]D. A. Goodings and V. Heine, Phys. Rev. Lett. 5, 370 (1960).
[24]R. E. Watson and A. J. Freeman, Phys. Rev. 123, 2027 (1961); A. J. Freeman and R. E. Watson, in *Magnetism*, edited by G. Rado and H. Suhl (Academic, New York, 1965), Vol. II, p. 167.
[25]P. S. Bagus and L. Liu, Phys. Rev. 148, 79 (1966).
[26]S. Wakoh and J. Yamashita, J. Phys. Soc. Jpn. 25, 1272 (1968).
[27]K. J. Duff and T. P. Das, Phys. Rev. B 3, 2294 (1971).
[28]K. J. Duff and T. P. Das, Phys. Rev. B 12, 3870 (1975).
[29]E. Clementi, *Tables of Atomic Functions* (IBM Corp., San Jose, 1965).
[30]C. E. Violet and D. N. Pipkorn, J. Appl. Phys. 42, 4339 (1971).
[31]C. Song, J. Trooster, and N. Benczer-Koller, Phys. Rev. B 9, 3854 (1974).
[32]T. Shinohara and M. Fujioka, Phys. Rev. B 7, 37 (1973).
[33]J. J. Mallow, A. J. Freeman, and J. P. Desclaux, Phys. Rev. B 13, 1884 (1976).
[34]M. B. Stearns, Phys. Rev. B 4, 4081 (1971); International Symposium on Perspectives for Hyperfine Interactions in Magnetically Ordered Systems by NMR and Other Methods, L'Aquila, Italy, Sept. 11–15, 1972 (unpublished, and private communication to N. Benczer-Koller).
[35]S. Wakoh and J. Yamashita, J. Phys. Soc. Jpn. 30, 422

(1971).
[36]P. D. DeCicco and A. Kitz, Phys. Rev. 162, 486 (1967).
[37]T. Paakkari and P. Suortti, Acta Crystallogr. A 22, 755 (1967).
[38]M. E. Radchenko and V. P. Tsvetkov, quoted by N. Sirota, Acta Crystallogr. A 25, 223 (1969).
[39]S. Hosoya, quoted by N. Sirota, see Ref. 38. A later citation (see Ref. 34) of unpublished work of this author with T. Fukumachi gives 18.44 ± 0.15 and 15.13 ± 0.99 for the form factors for the (110) and (200) reflections.
[40]B. W. Batterman, D. R. Chipman, and J. J. DeMarco, Phys. Rev. 122, 68 (1961).
[41]M. Diana and G. Mazzone, Phys. Rev. B 9, 3898 (1974).
[42]O. Terasaki, Y. Uchida, and D. Watanabe, J. Phys. Soc. Jpn. 39, 1277 (1975).
[43]J. J. DeMarco and R. J. Weiss, Phys. Lett. 18, 92 (1965).
[44]C. G. Shull, quoted by DeCicco and Kitz, see Ref. 36.
[45]D. R. Baraff, Phys. Rev. B 8, 3439 (1973).
[46]A. V. Gold, L. Hodges, P. T. Panousis, and D. R. Stone, Intern. J. Magnetism 2, 357 (1971).
[47]R. V. Coleman, R. C. Morris, and D. J. Sellmeyer, Phys. Rev. B 8, 317 (1973).
[48]M. M. Angadi, E. Fawcett, and M. Rasolt, Phys. Rev. Lett. 32, 613 (1974).
[49]J. Rath, C. S. Wang, R. A. Tawil, and J. Callaway, Phys. Rev. B 8, 5139 (1973).
[50]W. C. Phillips and R. J. Weiss, Phys. Rev. B 6, 4213 (1972).
[51]T. Paakkari and S. Manninen, Phys. Rev. B 8, 3765 (1973).
[52]L. Lam and P. M. Platzman, Phys. Rev. B 9, 5122 (1974).